Supporting Information

Matthews et al. 10.1073/pnas.1710733114

SI Materials and Methods

Experimental Organisms. Symbiotic Aiptasia ($n \sim 700$) were harvested from a long-term laboratory stock of the clonal population NZ1 (Aiptasia Population Genetics) and maintained in 0.22 μm aerated filtered seawater (FSW). Temperature was maintained at 25 °C with light provided by AQUA-GLO T8 fluorescent bulbs at ∼95 μmol photons m^{-2} s^{-1} (light: dark = 12 h:12 h). Anemones were fed twice a week with freshly hatched *Artemia* sp. *nauplii*.

Anemones were rendered aposymbiotic following the menthol-bleaching procedure (53). Whole anemones ($n = 20$) from the bleaching treatment were examined by confocal microscopy (Olympus Provis AX70, at 100× magnification) to detect the chlorophyll autofluorescence of any residual dinoflagellates. Anemones were selected at random and placed in a "relaxation" solution (50% 0.22 μm FSW and 50% 0.37 M $MgCl_2$) for 15 min before being moved to a FluoroDish glass-bottom confocal dish (World Precision Instruments). The autofluorescence emission of the *Symbiodinium* cells was excited using a 559-nm laser and captured at 647 ± 10 nm to confirm the aposymbiotic state of the anemones.

Two different *Symbiodinium* cultures were used: the homologous type *S. minutum* (ITS2 type B1) originally isolated from the laboratory Aiptasia stock (NZ1), and a heterologous type *S. trenchii* (ITS2 type D1a; culture I.D. Ap2). *Symbiodinium* cells were subcultured from laboratory stock and grown in silica-free f/2 medium (AusAqua Pty) for 6 wk before use in the colonization study. Cultures were grown at 25 °C and in light provided by cool white fluorescent lamps (18 W 840; Phillips), at an irradiance of 100 μmol photons m^{-2} s^{-1} with a 12-h:12-h light:dark photoperiod.

Inoculation of Aposymbiotic Aiptasia with *Symbiodinium*. Aposymbiotic anemones ($n \sim 220$ per treatment) were starved for 7 d before inoculation. One drop of *Symbiodinium* cells at $\sim 3 \times 10^6$ cells mL^{-1} was placed onto the oral disk of each anemone (except for the aposymbiotic treatment where a drop of 0.22 μm FSW only was used), followed by a dilute suspension of *Artemia* sp. *nauplii* to enhance phagocytosis. The aposymbiotic anemones were exposed to *Symbiodinium* cells for 24 h before the FSW was changed. This colonization procedure was repeated for another 3 wk (i.e., 4 wk total), during which the temperature and light regimes were maintained as per precolonization; however, the anemones were only fed during the symbiont colonization procedure so as to encourage symbiont uptake. Before sampling, anemones were starved for 1 wk, at which point they were sampled for transcriptomic and metabolomic analyses (i.e., 5 wk after the initial inoculation); symbiont density and genotype were also confirmed at this point (Symbiont Density and Symbiont Community Identification from Host Samples). This procedure allowed the two symbiont species to establish a symbiosis with similar densities, and confirmed that these two species persisted in the host Aiptasia beyond the 4-wk inoculation period.

RNA and Metabolomics Sampling. For each of the five replicate samples for each treatment, anemones were allocated into transcriptomic ($n = 10$ anemones) and metabolomic ($n = 30$ anemones) subsamples. Samples were obtained midway through the light cycle. RNA samples were collected through the addition of 50 mL of an RNA stabilizing buffer (3.5 M ammonium sulfate, 1 M sodium citrate, and 0.5 M EDTA, pH 5.2; recipe available at sfg.stanford.edu/recipe.html) and left overnight at 4 °C before being stored at −80 °C. For metabolite profiles, the seawater was gently discarded from each replicate and flash-frozen in liquid nitrogen to quench the metabolism (∼10 s). Samples were stored at −80 °C until processing.

RNA Extraction. Total RNA was extracted and purified from the tissues of individual anemones, selected at random from each frozen sample ($n = 3$ individual anemones per sample per treatment), using a combination of the TRIzol RNA isolation (Life Technologies) and RNeasy Mini Kit (Qiagen) protocols. Extracted RNA was DNase-treated using an Ambion TURBO DNA-Free Kit (Thermo Fisher Scientific) according to the manufacturer's instructions. RNA quantity and quality were assessed using a NanoDrop ND-1000 UV-Vis spectrophotometer (Thermo Fisher Scientific) and gel electrophoresis. Samples containing <1 μg of total RNA were excluded from the analysis. From the remainder, a single extraction with the highest RNA quality was selected per sample per treatment for further analysis ($n = 5$ per treatment).

Preparation of cDNA for Illumina Sequencing. From each sample, 1 μg of total RNA was heat-fragmented at 95 °C for 10 min. cDNA libraries were synthesized following a 3′ tag-based RNA-Seq protocol as described previously (54). Individual cDNA libraries were labeled with sequence-specific barcode adaptors, and final cDNA samples ranging in size from 250 to 350 bp were excised from a 2% agarose gel.

Sequencing, Processing, and Mapping. cDNA libraries were pooled and sequenced in a single lane on an Illumina HiSeq 2000 sequencing system. Single-end sequencing of 15 cDNA libraries produced 100-bp-long reads. Sequences were de-multiplexed based on their sample-specific barcode adaptors. Raw sequences were filtered and trimmed using custom Perl scripts (https://github.com/Eli-Meyer) to remove uninformative (i.e., adaptor sequences, homopolymer repeats) or low-quality (>20 positions with a quality score <20) reads. High-quality reads were mapped to the reference transcriptome using SHRiMP version 2.2.2.

RNA-Seq Reference Transcriptome Assembly and Annotation. A concatenated transcriptome made up of both Aiptasia and *Symbiodinium* clade B transcriptomes was assembled for mapping of raw reads. The *Symbiodinium* transcriptome was included to separate the *Symbiodinium* genes from Aiptasia genes in the downstream analyses. The reference transcriptome for *A. pallida* was assembled using raw reads provided by Erik Lehnert, University of Wisconsin–Madison (now available as SRA accession no. SRX231866). Before assembly, the raw reads were processed to remove low-quality or uninformative reads using custom Perl scripts (https://github.com/Eli-Meyer). Any reads with >30 positions with low-quality scores (Phred score <20), and any reads matching the adaptors used in library construction (cross-match score >15) were removed. The cleaned high-quality reads were then assembled using the de novo transcriptome assembler Trinity version 2.0.2 (trinityrnaseq_r2012-06-08) with default settings. The assembly was annotated based on sequence comparisons to public sequence databases using BLAST (National Center for Biotechnology Information). Each transcript was assigned a gene name via a comparison against UniProt protein sequence databases (SwissProt and TREMBL version 2012_09), using BLASTx (e-value $<10^{-4}$). Gene names were based on best matches, excluding uninformative identifiers. The final concatenated reference transcriptome has been deposited in the Dryad database (www.datadryad.org/).

Identification of DE Genes. All statistical tests were conducted using R version 3.2.1. Statistical comparisons of RNA-Seq count data among the three symbiotic states were completed using the R package DESeq2 version 1.9. DESeq2 was selected for differential expression analysis because it uses a variance-stabilizing procedure to transform count data into weighted expression values suitable for linear modeling. Raw *P* values were adjusted for multiple test corrections and false discovery rate (FDR) using the Benjamini–Hochberg procedure, and a transcript was considered DE if the resulting adjusted *P* value was <0.1, the default setting in DESeq2. Differential expression was also examined using an FDR <0.05, but considering the low number of DE genes, an adjusted *P* value < 0.1 was used for the final analysis (Table S1). Gene expression heat maps were created with the *pheatmap* package in R version 3.1.3.

Functional Summaries. Annotated transcripts were assigned a GO molecular function using BLAST2GO Pro version. 3.2.7 and a manual search of the Uniprot database, and grouped into putative functional categories based on literature and database searches.

Aiptasia Population Genetics. To evaluate whether all samples used for gene expression analysis were clonal (i.e., produced from asexual reproduction), we analyzed sequence variation in RNA-Seq data. For this analysis, we started with the same alignments used for gene expression analysis, further filtering these to exclude any read with more than two mismatches to the reference. To handle the enormous variation in coverage inherent to RNA-Seq data (>1.1-million-fold difference in abundance between the most highly expressed gene and the lowest), we excluded low-coverage loci (<20×) where genotypes cannot be confidently assigned due to sampling error.

To eliminate genotyping errors arising from excessive coverage in highly expressed genes, we randomly sampled 100 reads from any genes with coverage >100×. We used samtools and bcftools to sort, index, and produce multiple sequence alignments (i.e., pileups) of reads against reference sequences. We initially planned to also use bcftools to call genotypes from these data, but preliminary analysis revealed that this software made numerous genotyping errors in these RNA-Seq data, failing to detect heterozygosity at loci with unequal allele frequencies (which may result from allele-specific expression or amplification bias during library preparation or sequencing). To account for this variation, we relaxed assumptions of equal allele frequencies, counting loci as homozygous if a second allele was present at <1% and as heterozygous if a second allele was present at ≥25%. Loci with intermediate allele frequencies were discarded for the same reason as loci with low coverage: genotypes cannot be confidently assigned at these positions. To evaluate whether samples were clonal, we further filtered the dataset to exclude loci genotyped in <50% of samples.

Sequence comparisons support the conclusion that the collection of anemones used for these experiments were clonal. Stringent filtering of RNA-Seq alignments for this analysis identified a set of 17,788 loci (base pairs) distributed across 361 genes. These genetic loci were sequenced at sufficient coverage (≥20×) for confident determination of genotypes in at least one half of the samples. In this relatively large SNP dataset, we found exactly zero polymorphisms, strongly supporting the conclusion that all anemones used in this experiment were genetically identical (i.e., clonal). For comparison, population comparisons of Aiptasia have revealed 1 SNP per 248 bp and 1 SNP per 808 bp. At those levels of polymorphism, we would expect to observe 22–71 SNPs in a dataset of this size. The probability of randomly drawing this number of monomorphic loci (17,788) at these SNP frequencies is exceptionally low ($P < 2.7e-10$), so we conclude that these animals were in fact clonal (as expected based on their prolific asexual reproduction in captivity).

Metabolite Sample Processing. All sample processing steps were performed at 4 °C. Frozen anemones were thawed on ice and then pooled into single samples ($n = 30$ anemones per sample per treatment) to ensure sufficient biomass for metabolite identification, and 500 μL of cold (4 °C) MilliQ water was added. Anemones were rapidly homogenized with a mechanical sawtooth homogenizer (IKA T10 BS5; Thermo Fisher Scientific) for 1 min at a midspeed setting. Once homogenized, 5 mL of cold (4 °C) MilliQ water was added, the sample was thoroughly vortexed, and a single 500-μL aliquot was removed for *Symbiodinium* cell density estimates. Symbionts were pelleted by centrifugation (2,500 × *g* for 5 min at 4 °C), and the host supernatant was transferred and diluted with 5 mL of cold MilliQ water, followed by vigorous vortexing for 1 min and then a second centrifugation (2,500 × *g* for 5 min at 4 °C) to remove residual symbiont cells. In subsamples ($n = 20$) of the host material, the absence of *Symbiodinium* was confirmed by light microscopy (at 40× magnification). The cleaned host fractions were frozen at −80 °C for 1 h and then lyophilized (FreeZone Plus 4.5-Liter Cascade; Labconco) for 18 h at −105 °C. Then 3 mL of cold (4 °C) MilliQ water was added to the symbiont pellets, the sample was gently vortexed to resuspend the cells, and a single 500-μL aliquot was obtained, to which 500 μL of DNA buffer (0.4 M NaCl and 0.05 M EDTA) with 1% (wt/vol) SDS was added. The samples were frozen at −20 °C for symbiont identification, and the remaining symbiont material was frozen at −80 °C.

Symbiont Density. The aliquot of the homogenate was centrifuged at 1,000 × *g* for 5 min to separate the animal and algal fractions. The host supernatant was collected, and the algal pellet was resuspended in 1 mL of FSW. *Symbiodinium* cell densities were quantified using a Neubauer improved blood counting chamber (Boeco), with a minimum of 10 replicate counts per sample (i.e., to a confidence interval <10%). Cell density was calculated by normalizing counts to the soluble protein content of the host supernatant, which was assessed by the Bradford assay, with BSA as the standard. To test for differences in *Symbiodinium* cell density between the *S. trenchii*- and *S. minutum*-colonized hosts, assumptions of normality and homoscedasticity were assessed using the Shapiro–Wilk and Levene tests, respectively. Because the data failed to meet the assumptions of normality, a nonparametric Mann–Whitney *U* rank-sum test was performed at the $P < 0.05$ probability level using SPSS version 20 (IBM).

Symbiont Community Identification from Host Samples. For specimens used in the RNA-Seq analysis, symbiont type was verified at the individual sample level (i.e., mRNA library level) by direct sequencing of clade-specific reads at three loci known to be highly divergent between clades: internal transcribed spacer regions 1 and 2 of ribosomal DNA (ITS1 and ITS2 rDNA), and chloroplast 23S rRNA (cp23S). cDNA synthesis was performed using the Invitrogen SuperScript III First-Strand Synthesis System for RT- PCR (Thermo Fisher Scientific) in accordance with the manufacturer's instructions using a random hexamer primer. The ITS1, ITS2, and cp23s regions were amplified using the outer primer combinations S-Dino (5′-CGCTCCTACCGATTGAGTGA-3′) and D1R-rev (5′-ACCCGCTGAATTTAAGCATAT-3′), ITSintfor2 (5′-GAATTGCAGAACTCCGTG-3′) and ITS2rev2 (5′-CCTCCGCTTACTTATATGCTT-3′), and cp23s1 (5′GCTGTAACTATAACGGTCC-3′) and cp23s2 (5′-CCATCGTATTGAACCCAGC-3′), respectively. Samples were sequenced on an ABI 3730 capillary sequencing machine (Applied Biosystems), and their identities were confirmed by reciprocal BLAST searches ($n = 5$).

For the metabolomics samples, direct sequencing of the ITS2 and cp23S regions was used to verify symbiont type. Symbiont pellets were preserved in 1% SDS, and DNA was extracted using a CTAB-chloroform extraction protocol (https://www.protocols.io/view/Bulk-gDNA-extraction-from-coral-samples-dyq7vv). Samples were immediately subjected to PCR analysis, using 1 μL of DNA template solution, 1× MyTaq PCR mix (Bioline), 10 pmol each primer (the aforementioned ITS2 and cp23s primers), and deionized sterile water to a total volume of 25 μL. Thermal cycling conditions included an initial denaturation step of 3 min at 95 °C, followed by 40 cycles of 15 s at 95 °C, 15 s at 56 °C, and 10 s at 72 °C. A template-free control was included with each run. PCR products were cleaned with ExoSAP-IT (USB Corporation) and sequenced by Macrogen. Sequences were aligned with Geneious v. 7.0 (Biomatters), and a BLAST search was carried out against *Symbiodinium* ITS2 and cp23s sequences in GenBank.

Intracellular Metabolite Extraction. Once thoroughly dry, 1 mL of 100% methanol (−20 °C) containing the internal standard alanine-2,3,3,3-d_4 (Sigma-Aldrich) was added to ∼30 mg of lyophilized host material to extract the semipolar metabolites. The host fractions were sonicated for 30 min at 4 °C in an ultrasonic bath (model 8854; Cole-Parmer) and centrifuged (3,000 × *g* for 30 min at 4 °C), and the supernatant containing the extracted metabolites was collected and stored at −80 °C. Extraction was then repeated with 1 mL of 50% MeOH (−20 °C) to extract the polar fraction. Samples were then centrifuged (3,000 × *g* for 30 min at 4 °C), and the supernatant was pooled with the first extract. The total extract was then further centrifuged at 16,100 × *g* for 15 min at 4 °C to ensure the removal of all particulates. Aliquots (total volume, 200 μL) were then concentrated under vacuum (Eppendorf Concentrator 5301) at 30 °C until dry. The cell debris was frozen at −20 °C for protein quantification, as determined by a modified Bradford colorimetric method.

Trimethylsilyl ester derivatization of sugars, sugar alcohols, and amino/nonamino acids for GC-MS was performed using an automated online derivatization, adapted from established protocols (55). In brief, all samples were redissolved in 20 μL of 30 mg mL^{-1} methoxyamine hydrochloride in pyridine and then derivatized at 37 °C for 120 min with mixing at 500 rpm. Then 20 μL of N,O-bis-(trimethylsilyl)trifluoroacetamide and 1 μL retention-time standard mixture composed of *n*-alkanes were added, and the samples were incubated for another 30 min with mixing at 500 rpm. Each derivatized sample was then allowed to rest for 60 min before GC-MS analysis. The GC-MS analysis was performed on an Agilent 7890 gas chromatograph equipped with a Gerstel MPS2 multipurpose sampler and coupled to an Agilent 5975C VL mass selective detector, run in splitless mode, with an injection volume of 1 μL of each sample and a technical replicate of two injections per sample. Instrument control was performed with Agilent G1701A Revision E.02.01 ChemStation software. The gas chromatograph was fitted with a Varian Factor 4 column (VF-5ms; 30 m × 0.25 mm × 0.25 μm + 10 m Ezi-guard). Helium (ultra-high purity) was in constant flow mode at ∼1 mL min^{-1} with retention-time locking applied. The oven temperature was started at 70 °C, held at this temperature for 1 min, and then increased at 7 °C min^{-1} to 325 °C and held at this temperature for 3.5 min.

The mass spectrometer quadrupole temperature was set at 150 °C, with the source set at 250 °C and the transfer line held at 280 °C. Positive ion electron impact spectra at 70 eV were recorded in scan mode with the following settings: gain factor of 1.00, detector threshold of 150, mass to charge (*m*/*z*) range of 50–600 *m*/*z*, and solvent delay of 6.0 min. Along with the samples, a series of known metabolite mixtures and solvent-only blanks were analyzed. The metabolite mixtures contained the major compound classes being targeted, including amino acids (Amino Acid Standard solution AAS18; Sigma-Aldrich), fatty acids (Menhaden fish oil; Sigma-Aldrich), and sugars (2.5 μM ribitol, ribose, fructose, glucose, arabinose, galactose, mannitol, xylose, mannose, and sucrose; Sigma-Aldrich), and were analyzed to confirm that these compounds could be accurately identified.

Metabolite Data Extraction, Preprocessing, and Normalization. Metabolite data extraction and analysis were performed with AMDIS (chemdata.nist.gov/mass-spc/amdis) and Agilent MassHunter Workstation software (Quantitative Analysis, vB.05.00/Build 5.0.291.0). Compound identification was based on an in-house library of MS spectra, with retention indices based on n-alkane and the amino acid, fatty acid and sugar standards. Derivative peak areas were used to quantify the concentrations of individual metabolites. Data were normalized to the final area of the internal standard alanine-2,3,3,3-d_4 and the protein content of the cell debris resulting from the sample's intracellular metabolite extraction, using a modified Bradford colorimetric method, to account for differences in the amount of lyophilized host material used in the extraction. Data were then tested for normality and homogeneity, and log2-transformed when necessary. Data were then autoscaled, and statistical analysis was performed using MetaboAnalyst 3.0 (www.metaboanalyst.ca). Relative metabolite concentrations were evaluated by PCA. To specifically investigate how *Symbiodinium* genotype affects host metabolism, the fold change in relative metabolite abundance was calculated between B1-colonized hosts and D1a-colonized hosts before autoscaling and log2 normalization. Metabolites were considered significantly different when the *t* test *P* value was <0.05 and the fold change was >2 for all five biological replicates. Visual exploration of the metabolites in the respective metabolic pathways was illustrated using Vanted version 2.6.2.

Pathway Analysis. For integrated pathway analyses, a joint Wilcoxon pathway enrichment analysis of transcriptomic and metabolomic data was performed using the IMPaLA web interface (56). Input data consisted of the fold change in expression of the variance-stabilized data of all Uniprot annotated genes (13,535 transcripts), and the log2 fold change in relative abundance between B1-colonized hosts and D1a-colonized hosts of the 85 metabolites with KEGG identifiers. Pathways were considered significantly affected if the FDR was <0.05, and pathways with fewer than three genes or metabolites measured were filtered out.

Fig. S1. GO categorization of DE genes ($P < 0.1$) across the three symbiotic states: heterologous *S. trenchii*-colonized, homologous *S. minutum*-colonized, and aposymbiotic hosts. Genes were assigned a GO molecular function and grouped into putative categories based on GO slimming and literature searches.

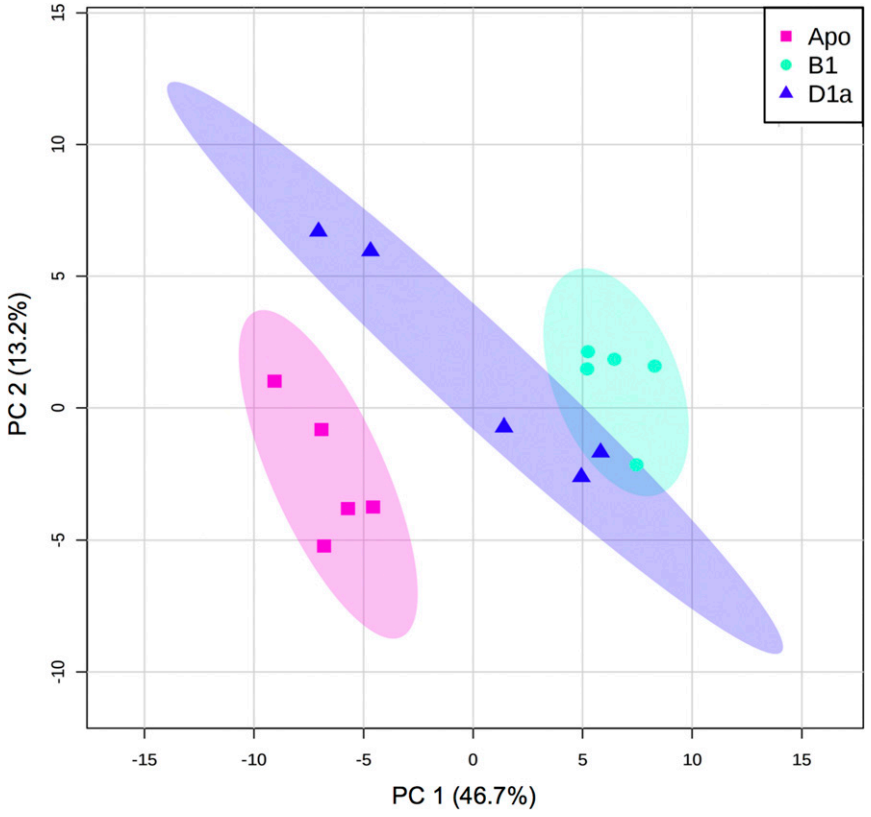

Fig. S2. Host metabolite profile PCA scores plot, with 95% confidence intervals. Shown is the relative abundance of the compounds detected in host free pools between the three symbiotic states, with 95% confidence regions ($n = 5$). Anemones are colonized by either homologous *S. minutum* (B1) or heterologous *S. trenchii* (D1a), or are aposymbiotic (Apo).

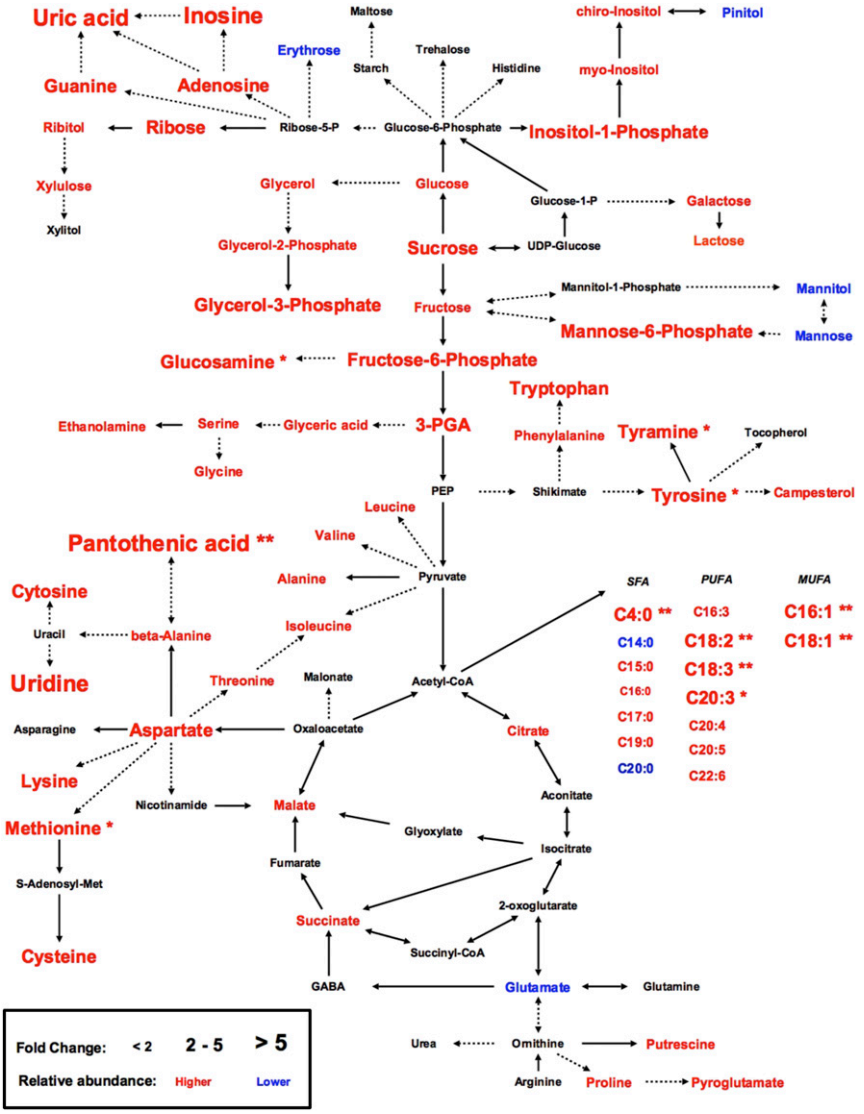

Fig. S3. Altered metabolic pathway activity in response to symbiont type. Aiptasia colonized with a heterologous symbiont (*S. trenchii*) were compared with those colonized with the homologous symbiont (*S. minutum*). Font size represents fold change of relative abundance in heterologous host pools compared with homologous host pools. Asterisks denote compounds that differed significantly (two-way ANOVA; $*P < 0.05$, $**P < 0.01$) between symbiont species. Font color indicates whether compound abundance was higher (red) or lower (blue) in heterologous host tissues, or represents metabolic intermediates not detected in the metabolite data (black).

Table S1. Transcriptome assembly, mapping, and differential expression statistical values

Variable	Value
De novo transcriptome assembly	
No. of reads after quality filtering	168,677
Total no. of contigs	63,789
Total subcomponent isogroups	58,160
Total after filtering for low counts per transcript	35,516
Average contig length, bp	840
Maximum contig length, bp	35,295
Minimum contig length, bp	40
N50 of all contigs, bp	1,449
Mapping	
Average no. of reads per sample after filtering	7,815,728
Differential expression	
No. of transcripts passing thresholds and tested for differential expression	35,516
No. of transcripts differentially expressed with symbiont type ($P < 0.05$)	514
No. of transcripts differentially expressed with symbiont type ($P < 0.1$)	720
No. of transcripts differentially expressed after symbiont transcripts removed	686
Percentage of differentially expressed transcripts with UniProt matches	60

Table S2. Summary of the main molecular processes differentially expressed across the three symbiotic states (homologous *S. minutum*-colonized, heterologous *S. trenchii*-colonized, and aposymbiotic anemones)

DE genes	N	Uniprot	Molecular function	*S. minutum*-colonized anemones	*S. trenchii*-colonized anemones	Aposymbiotic anemones
Binding	23					
Calmodulin binding		F1A0N9	Calcium ion binding	−0.007	0.028	−0.021
CnidEF ($n = 2$)		Q2ESH8	Calcium ion binding	−0.091	−0.003	0.088
Catalytic/enzymatic activity	48					
TauD		B7JWG7	Sulfur transferase enzyme	0.104	0.046	−0.163
Cell cycle	70					
E3 ubiquitin-protein ligase		Q4KLN8	Protein modification	−0.038	0.025	0.012
Molecular chaperone		B7Q4C2	Protein modification	0.057	−0.034	−0.024
Ubiquitin domain-containing protein		Q54MD2	Protein modification	−0.087	−0.033	0.112
Cytoskeleton	35					
Actin binding protein		Q8H1L9	Actin binding	0.051	−0.010	−0.042
Actin binding protein		Q6WE55	Actin binding	0.148	−0.260	0.080
Actin binding protein		P28575	Actin binding	0.082	−0.060	−0.026
Beta gamma crystallin isoform 8		A8C9L8	Cytoskeletal protein binding	−0.002	−0.067	0.065
Echinonectin		O76470	Cytoskeletal protein binding	0.050	−0.075	0.022
Nectin		Q70JA0	Cytoskeletal protein binding	0.063	−0.062	−0.004
Extracellular matrix	21					
Collagen trimer alpha-1(III)		Q08E14	Collagen binding	−0.065	0.017	0.046
Collagen trimer alpha-1(XI)		Q61245	Collagen binding	−0.053	0.010	0.042
Collagen trimer alpha-1(I)		Q9YIB4	Collagen binding	−0.060	0.014	0.044
Collagen trimer alpha-5(VI) ($n = 2$)		G3GZJ0	Collagen binding	−0.071	0.023	0.045
Metabolism	62					
Arginine kinase activity		O15992	Amino acid metabolism	−0.054	0.042	0.010
Ornithine decarboxylase antizyme		B2CR15	Amino acid metabolism	0.055	−0.022	−0.034
Phenylalanine tRNA synthetase		Q5EBG3	Amino acid metabolism	−0.014	−0.046	0.059
Proline catabolism		Q4V7V6	Amino acid metabolism	−0.073	0.027	0.043
Serine/threonine protein kinase		F2ULY7	Amino acid metabolism	−0.019	−0.022	0.040
Carbohydrate metabolism		A3HS07	Carbohydrate metabolism	−0.102	0.026	0.070
Carbohydrate metabolism		I3IDI2	Carbohydrate metabolism	−0.117	0.010	0.099
Glycophosphatidylinositol-linked carbonic anhydrase		A3FFY2	Carbohydrate metabolism	0.100	−0.063	−0.042
Polysaccharide lyase activity		F0S761	Carbohydrate metabolism	−0.021	−0.077	0.093
Long-chain fatty acyl-CoA synthetase 1 (ACSL 1)		E2D780	Fatty acid metabolism	0.066	−0.023	−0.045
Cytosolic phospholipase A2		A4IFJ5	Arachidonic acid metabolism	−0.037	0.034	0.002
Phospholipase A2		A7LCJ2	Arachidonic acid metabolism	−0.100	0.018	0.077
Cryptochrome 2		A2I2P0	Gluconeogenesis	0.051	−0.016	−0.036
Lipase		A7SL62	Lipid metabolism	−0.052	0.019	0.031
Lipoxygenase		F2Z929	Lipid metabolism	−0.160	0.060	0.087
Phosphatidylinositol-specific phospholipase		D4A4P6	Inositol-phosphate metabolism	0.048	−0.011	−0.038
Triglyceride lipase		B3VMK3	Lipid metabolism	−0.154	0.041	0.102
Carboxypeptidase A2 ($n = 2$)		P48052	Protein metabolism	−0.092	−0.015	0.100
Carboxypeptidase B		E6ZIX2	Protein metabolism	−0.132	0.025	0.097
Carboxypeptidase D		E0VR63	Protein metabolism	−0.115	0.048	0.061
S-adenosylmethionine synthase		A7RTZ9	S-Adenosylmethionine synthase activity	0.086	−0.016	−0.074
S-adenosylmethionine synthase		A7SEP5	S-Adenosylmethionine synthase activity	−0.066	0.064	−0.001
Niemann–Pick disease C2		Q53HV6	Sterol metabolism	−0.051	0.012	0.038
Arginine translocation pathway signal		Q476C5	Urea cycle	−0.055	−0.026	0.077
Glutamate dehydrogenase		A7SE06	Urea cycle	−0.089	0.032	0.053
Stress response	58					
Apoptosis		Q5PQ83	Apoptosis	−0.032	0.058	−0.028
Apoptosis		B4DGI3	Apoptosis	−0.004	−0.029	0.032
Caspase 8		Q2LGB8	Apoptosis	−0.090	0.040	0.046
Fibroblast growth factor receptor		Q60818	Apoptosis	−0.046	−0.030	0.073

Table S2. Cont.

DE genes	N	Uniprot	Molecular function	*S. minutum*-colonized anemones	*S. trenchii*-colonized anemones	Aposymbiotic anemones
Oxidative stress induced growth inhibitor		Q2KIN7	Apoptosis	−0.065	0.035	0.028
TNF receptor 2		A2TK67	Apoptosis	−0.101	0.035	0.061
TNF receptor 3		A2TK68	Apoptosis	−0.120	−0.030	0.138
TNF receptor 6		A2TK70	Apoptosis	−0.012	−0.075	0.082
Tumor suppression gene		Q6VQ14	Apoptosis	−0.070	0.035	0.032
Cytochrome P450		A7TVD1	Cytochrome activity	0.367	−0.264	−0.189
Cytochrome P450		O42457	Cytochrome activity	0.121	−0.078	−0.051
Cytochrome P450		G7K3L7	Cytochrome activity	0.100	−0.205	0.085
ER stress associated protein		F1QWT4	ER Stress response	−0.052	0.039	0.011
ER stress associated protein		Q0V9K8	ER Stress response	−0.038	0.030	0.008
Glutamate-cysteine ligase catalytic subunit		B2ZG39	Glutathione synthase activity	−0.059	−0.001	0.058
GSS		Q5XJT8	Glutathione synthase activity	−0.029	−0.006	0.034
Glutathione peptidase		Q4PMF0	Glutathione synthase activity	−0.114	0.043	0.065
Cytosolic GST-2		B2ZI37	Glutathione transferase activity	−0.061	0.012	0.047
GST		C0NY90	Glutathione transferase activity	−0.080	0.038	0.038
DNAJ C3		Q7ZWH5	Heat shock	0.075	−0.030	−0.048
DNAJ C3		Q9ZWK3	Heat shock	−0.128	0.054	0.067
Macrophage expressed protein		F8RU73	Immune response	0.030	−0.089	0.055
Oxidoreductase		A7RUM6	Oxidoreductase activity	0.083	−0.041	−0.046
Redox enzyme		Q2KHP7	Oxidoreductase activity	−0.067	0.044	0.020
Sulfiredoxin-1		E0VWL8	Oxidoreductase activity	−0.161	0.100	0.048
Xanthine dehydrogenase		Q6NS03	Oxidoreductase activity	−0.106	0.048	0.052
Xanthine dehydrogenase		F4WWU5	Oxidoreductase activity	−0.042	0.036	0.005
Coenzyme Q6		Q6DF46	Oxidoreductase activity	−0.044	0.035	0.008
Protein disulfide isomerase		Q7PM55	Redox homeostasis	0.046	−0.024	−0.023
Thioredoxin domain-containing protein		Q7TN22	Redox homeostasis	0.049	−0.022	−0.029
Transport	48					
ABCD4		O14678	ABC transporter activity	0.061	−0.037	−0.026
Monocarboxylate membrane transporter		E0VFK5	Amino acid transport	−0.050	0.055	−0.008
Monocarboxylate membrane transporter (SLC16A10)		A1L1W9	Amino acid transport	−0.062	0.038	0.022
Monocarboxylate membrane transporter (SLC16A10)		Q3U9N9	Amino acid transport	−0.053	0.050	0.001
G protein coupled receptor		B2RXV6	Cellular signaling	−0.070	0.014	0.053
G protein signaling protein		A5PLK6	Cellular signaling	−0.037	0.128	−0.101
Lipid transport activity		F4WT31	Lipid transport	−0.222	0.058	0.140
Nonspecific lipid-transfer protein		O62742	Lipid transport	−0.056	0.029	0.025
Phosphatidylinositol signaling		F2Z2U4	Phosphatidylinositol signaling	0.048	−0.032	−0.017
Phosphatidylinositol signaling		E9CCM6	Phosphatidylinositol signaling	−0.039	0.015	0.023
Sodium phosphate cotransporter (SLC34A2)		Q9PT83	SLC transporter activity	−0.048	0.013	0.034
Transmembrane transport protein (SLC25A22)		Q6P4S3	SLC transporter activity	−0.123	0.061	0.054
Zinc transporter (SLC39A10)		Q9ULF5	SLC transporter activity	−0.098	0.044	0.050
Macrophage mannose receptor		Q2HZ94	Sugar transport	0.095	−0.081	−0.019
Sugar phosphate exchanger 2 (SLC37A2)		Q9WU81	Sugar transport	0.046	−0.046	−0.002

DE genes were assigned a GO molecular function and grouped into putative categories based on GO slimming and literature searches. Total number (N) for each category is provided. Log2 fold change is relative to the gene's mean for each treatment, and color indicates up-regulated (red) and down-regulated (blue) expression. Data are from Dataset S3.

Other Supporting Information Files

Dataset S1 (XLSX)
Dataset S2 (XLSX)
Dataset S3 (XLSX)
Dataset S4 (XLSX)
Dataset S5 (XLSX)
Dataset S6 (XLSX)